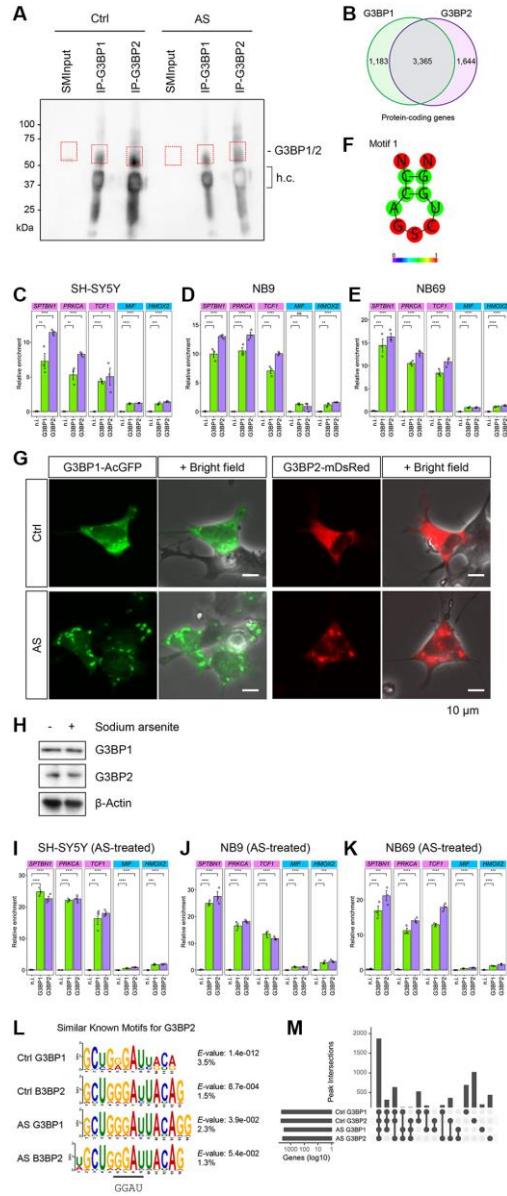
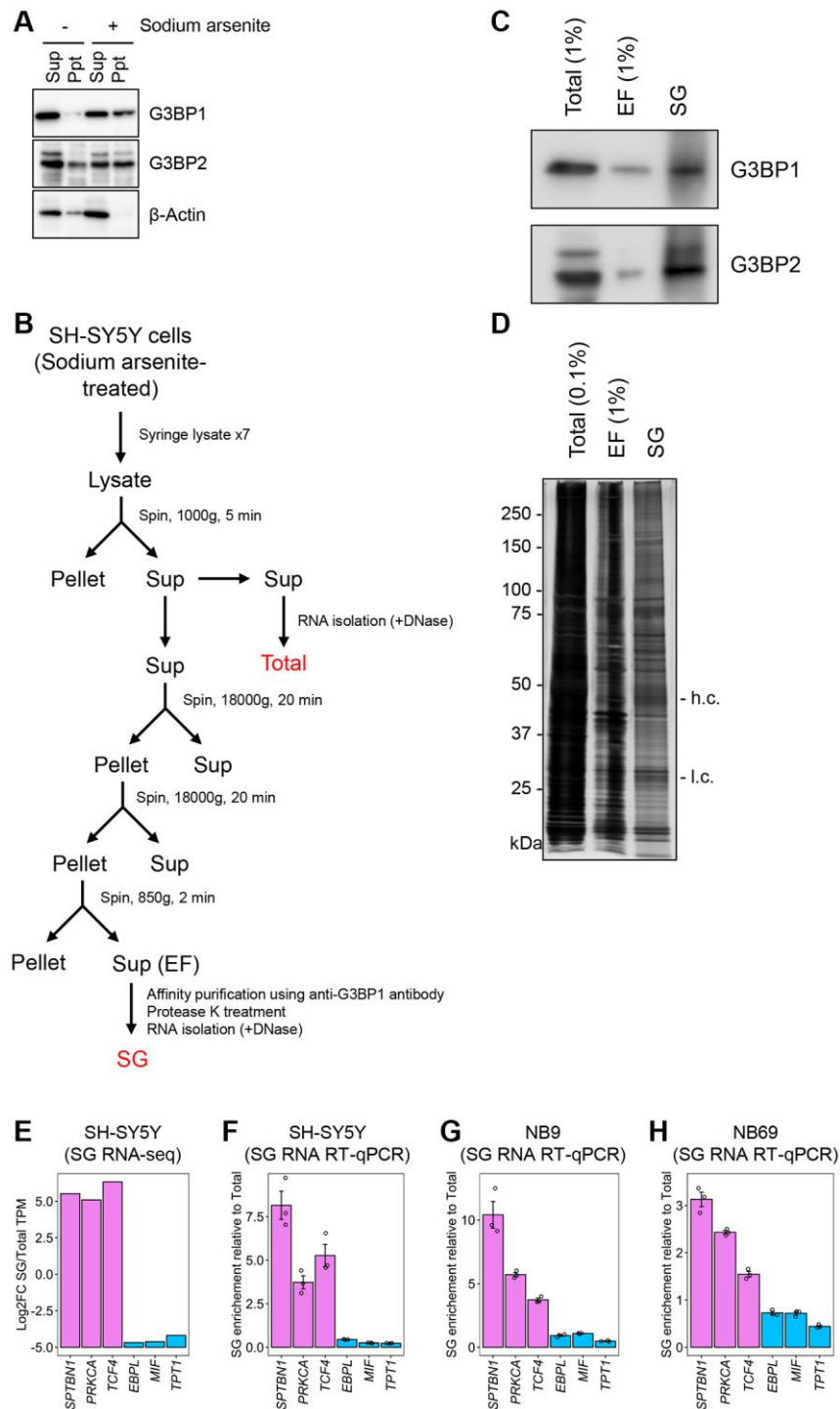


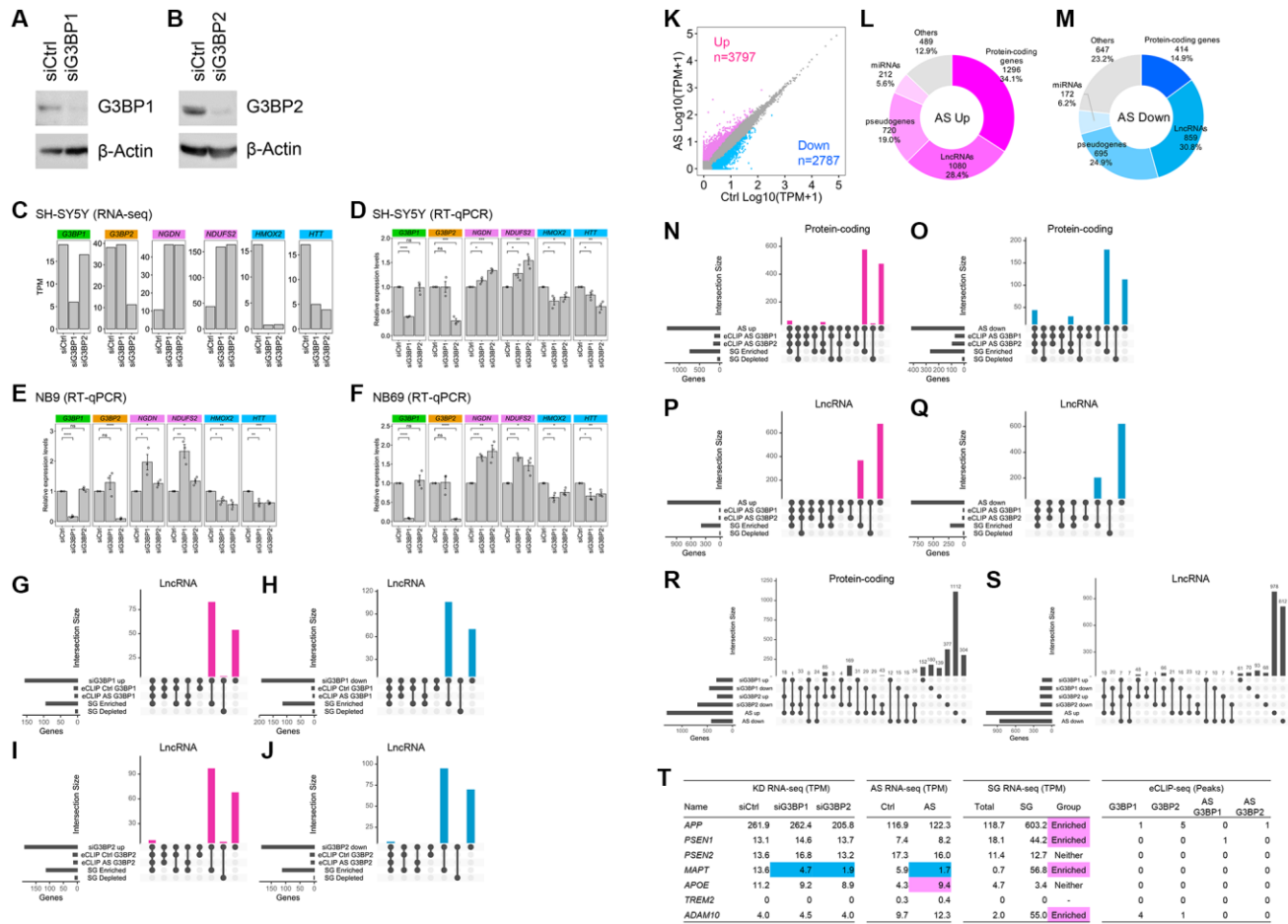
SUPPLEMENTARY FIGURES



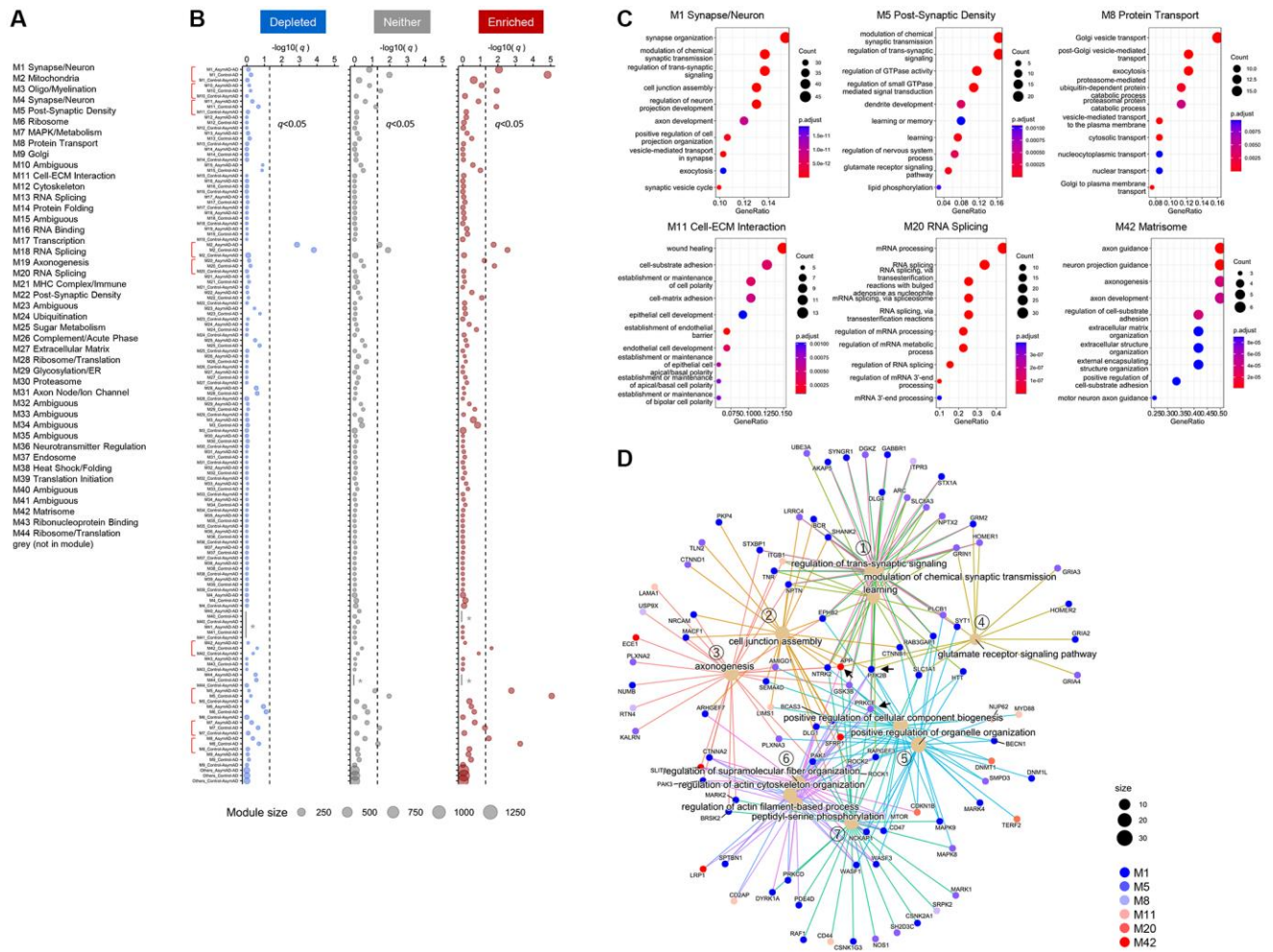
Supplementary Figure 1. Related to Figures 1 and 2. eCLIP-seq of 3BP1 and G3BP2 in SH-SY5Y cells. **(A)** Western blotting against immunoprecipitated (IP) G3BP1 and G3BP2 proteins before and after sodium arsenite (AS) treatment, confirming that both proteins were efficiently immunoprecipitated. SMInput is the size-matched input control. Red dotted squares indicate the gel-extracted regions for eCLIP-seq libraries. **(B)** Venn diagram depicting the overlapped mRNAs that possess G3BP1 and G3BP2 eCLIP-peaks. **(C–E)** Bar charts depicting the interaction between G3BP proteins and *SPTBN1*, *PRKCA*, *TCF4*, *MIF*, and *HMOX2* RNAs by RIP in SH-SY5Y **(C)**, NB9 **(D)**, and NB69 cells **(E)**. n.i.: non-immune IgG used as an IP negative control. Error bars represent standard error (SE) from three independent experiments. Statistical significances were assessed by Student’s *t*-test. ns: not significant, **p* < 0.05, ***p* < 0.01, ****p* < 0.001, *****p* < 0.0001. **(F)** Predicted RNA structure for motif 1 by CentroidFold. The color bar represents the probability of a base pair. S and N indicate G/C and any ribonucleotides, respectively. **(G)** Live imaging showing the cellular localizations of G3BP1-AcGFP and G3BP2-mDsRed in SH-SY5Y before (Ctrl) and after (Arsenite) sodium arsenite treatment. **(H)** Western blotting of G3BP1 and G3BP2 before and after AS treatment, indicating that the protein levels of G3BP1 and G3BP2 were unchanged by AS. **(I–K)** Bar charts depicting the interaction between G3BP proteins and *SPTBN1*, *PRKCA*, *TCF4*, *MIF*, and *HMOX2* RNAs by RIP in SH-SY5Y **(I)**, NB9 **(J)**, and NB69 cells **(K)** under stress condition. n.i.: non-immune IgG used as an IP negative control. Error bars represent SE from three independent experiments. Statistical significances were assessed by Student’s *t*-test. ***p* < 0.01, ****p* < 0.001, *****p* < 0.0001. **(L)** Similar known motif for G3BP2 [36] enriched within eCLIP-peaks of G3BP1- and G3BP2-bound RNAs. **(M)** Intersection across mRNAs that possess G3BP1 and G3BP2 eCLIP-peaks.



Supplementary Figure 2. Related to Figure 3. Isolation of SG cores in SH-SY5Y cells. **(A)** Western blotting of G3BP1 and G3BP2 following cellular fractionated SH-SY5Y cells before and after sodium arsenite treatment. Sup, supernatant; ppt, precipitate. Actin was used as a marker for cytoplasm. **(B)** Schematic representation of the SG purification process in SH-SY5Y cells. In brief, after SG formation induced by sodium arsenite, SH-SY5Y cells were subjected to syringe lysis, followed by a series of centrifugation steps. The SG cores were then affinity purified using anti-G3BP1 antibody and treated with proteinase K. RNA was isolated via ISOGEN II extraction, yielding purified SG core RNA. EF, SG-enriched fraction; SG, SG cores. **(C)** Western blotting of G3BP1 and G3BP2 following affinity purification of SG cores. **(D)** Silver staining following affinity purification of SG cores. **(E–H)** Bar charts depicting Log2-fold change of SG/Total TPM scores for the indicated genes in SG RNA-seq data. **(F–H)** Bar charts depicting the relative RNA levels of the indicated genes in SG cores determined by RT-qPCR in SH-SY5Y **(F)**, NB9 **(G)**, and NB69 cells **(H)**. Error bars represent SE from three independent experiments.

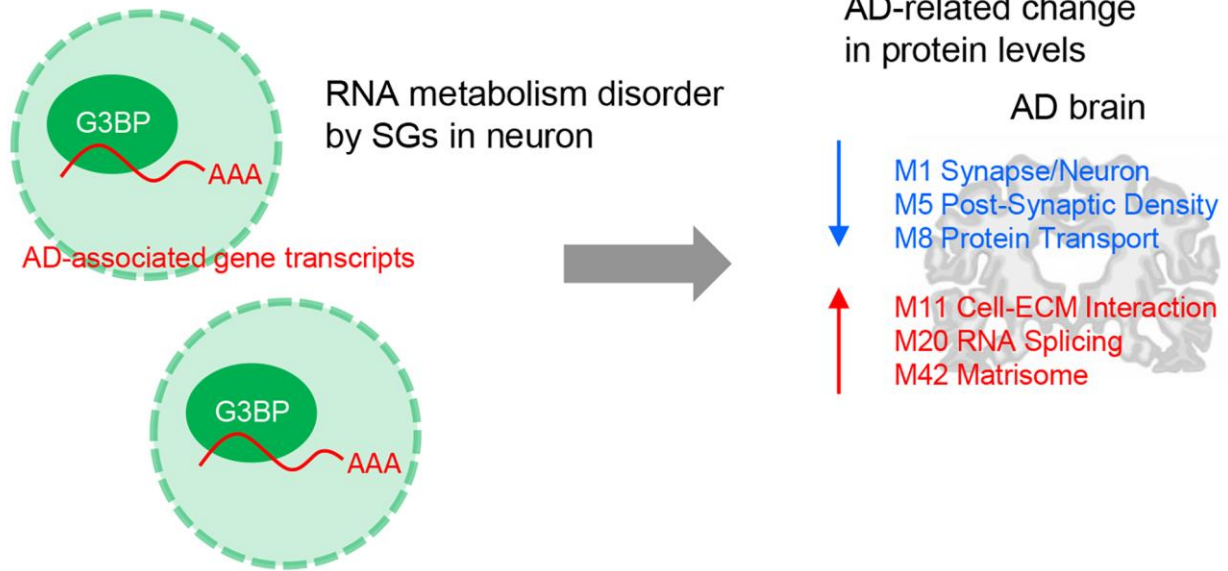


Supplementary Figure 3. Related to Figure 6. Changes in RNA levels upon the depletion of G3BP1 and G3BP2, and AS treatment in SH-SY5Y cells. (A, B) Western blotting of G3BP1 (A) and G3BP2 (B) in G3BP1- and G3BP2-depleted SH-SY5Y cells, respectively. (C) TPM scores of G3BP1 and G3BP2 in control (siCtrl), G3BP1-depleted (siG3BP1), and G3BP2-depleted (siG3BP2) cells. (D–F) Bar charts depicting changes in RNA levels of the indicated genes determined by RT-qPCR in G3BP1 and G3BP2-depleted SH-SY5Y (D), NB9 (E), and NB69 cells (F). Relative expression levels were calculated by normalizing to *GAPDH*. Error bars represent SE from three independent experiments. Statistical significances were assessed by Student's *t*-test. ns: not significant, **p* < 0.05, ***p* < 0.01, ****p* < 0.001, *****p* < 0.0001. (G–J) Intersections across upregulated, downregulated genes upon knockdown, and enriched RNAs based on eCLIP-seq and SG RNA-seq of LncRNAs. (K) Scatter plot depicting RNA abundance in AS-treated cells. (L, M) Pie charts depicting the relative contribution of gene categories for upregulated (L) and downregulated (M) genes upon AS-treatment. (N–Q) Intersections across upregulated and downregulated genes upon AS-treatment and enriched RNAs based on eCLIP-seq and SG RNA-seq of protein-coding genes and LncRNAs. (R, S) Intersections for upregulated or downregulated genes of protein-coding genes (R) and LncRNAs (S) upon knockdown and AS-treatment. (T) RNA levels of major AD risk factors upon depletion of G3BP1 and G3BP2, AS treatment, enrichment to SG, and G3BP1 and G3BP2 eCLIP-peaks. Red and blue backgrounds indicate upregulated and downregulated genes, respectively. SG-enriched genes were also indicated with red background.



Supplementary Figure 4. Related to Figure 7. Association between SG-enriched RNAs and changes in protein levels in AD brains. (A) List of 44 protein co-expression modules modified from Johnson et al. [47]. (B) Correlation between SG-enriched RNA levels and Module eigenprotein levels. Differences of protein expression level by case status in each module were assessed by one-way ANOVA with Tukey test and shown as $-\log_{10}(q)$ -value. The dashed lines indicate $q = 0.05$, above which enrichment was considered significant. The red square brackets indicate nine modules containing sets that showed significant changes in protein levels in SG-enriched, depleted, or “Neither” groups. Asterisks (*) indicate no proteins included. (C) GO analysis for SG-enriched genes classified in each module. (D) Gene-Concept Network analysis for SG-enriched AD-associated genes classified in six modules.

Stress granules (SGs)



Supplementary Figure 5. A model for the mechanism of sequestration of AD-associated gene transcripts by SGs and its impact on disease-related proteomic changes. SGs sequester RNAs, which consequently cause changes in protein levels of six modules associated with the development of AD.